to PEIT because it requires only one session to achieve complete necrosis (6, 7). Although RFA was initially expected to decrease the incidence of local recurrence, recent reports indicate that local recurrence after RFA is not uncommon (8–12). Furthermore, in some cases, the recurrence was rapid and vessel-invasive (13, 14). The recurrence in RFA seems unusual because thermal ablation is considered to achieve complete necrosis readily, regardless of intra-tumor septa.

Because explosive sounds are often heard during the RFA procedure, it is feared that rapid heating of a tumor may lead to an unpredicted increase in internal pressure and this might cause the dislodgement and scattering of malignant cells around the ablated tumor; however, there is no direct evidence that the high internal pressure RFA attributed to local recurrence. To confirm this hypothesis, we measured the intra-hepatic pressure during RFA using a model comprising a liver block sealed within a rigid plastic case. Although we neglected the influence of blood flow in this model, it was considered to be similar to a well-encapsulated HCC tumor. In addition to comparing the various conditions for ablation, we tried to optimize the procedure to reduce ablation time and to avoid increases in pressure.

Materials and methods

Measurement of ablation time and pressure *in vitro* model

Pig livers were prepared for the ablation studies 6 h after sacrifice. Two blocks of liver tissue ($5 \times 5 \times 4\,cm^3$) were cut and packed into a rigid $5 \times 5 \times 8\,cm^3$ plastic case with a pressure sensor (model P303-01, M0101D; SSK Co., Ltd., Tokyo, Japan) mounted at one end (Fig. 1). The case containing the pig liver was cooled on ice for 15 min before ablation in order to maintain constant conditions. We used a LeVeen® needle, an expansion-type electrode with 10 tines in an umbrella pattern, as the device for RFA (3.0 cm type; Boston Scientific Corporation, Natick, MA, USA) and supplied the electric current from a generator (model RF2000®: Boston Scientific Corporation). In this apparatus, the resulting increase in tissue resistance to current flow (impedance) is measured in ohms, and when the impedance reaches a programmed end point, the current is automatically shut off. At the programmed end point of the ablation (roll-off), clinically sufficient necrosis is achieved.

As shown in Fig. 1, the electrode needle was inserted from the opposite end of the apparatus to the pressure sensor, until the tip of the needle

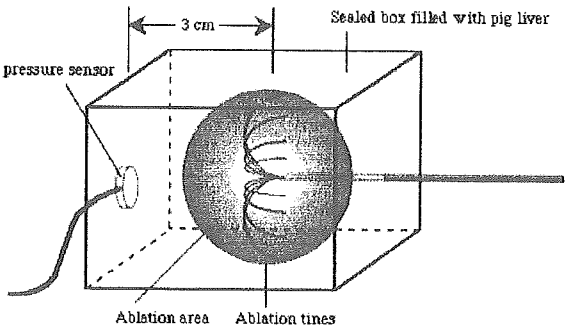

Fig. 1. The system for measuring pressure during ablation is shown. A block of pig liver was compactly packed into a rigid plastic case. A pressure sensor was located at the one end of the case, and the electrode needle was inserted from the opposite end until the tip of the needle was 3 cm from the sensor.

reached 3 cm from the sensor. For analysis of the single-step method, the pressure was measured every 20 s until complete ablation (roll-off) was achieved. The pressure at the programmed end point was also measured. The multi-step method also was examined using this pressure-measuring system. The stepwise expansion was performed using two different procedures: four steps and 10 steps. In the four-step method, a quarter of the length of the electrode tines was expanded for the first step and the current was delivered until roll-off was achieved. Next, half the length of the tines was expanded for the second-step and the current was supplied. For the third and final steps, the tines were expanded to three quarters of their full-length. Similarly, in the 10-step method, the tines were expanded by one-tenth of their length at each step, up to complete expansion for the final-step, and roll-off was achieved at each step. In the 10-step method, the ablation was performed at 30, 50 and 70 W, and the time to achieve roll-off and the pressure at the programmed end point were recorded at each step. In order to confirm the change in cell density under the ablation pressure, the histological findings in the pig liver were examined by hematoxylin and eosin (H&E) staining after single- and four-step ablation.

Measurement of ablation time in clinical HCC cases

We performed a preliminary comparison of ablation times for the single- and multi-step methods in 20 HCC cases with liver cirrhosis (Table 1). For the single-step method ($n = 10$), ablation was started at 50 W, and the electrical power was increased by 10 W/min in the subsequent ablation until 90 W was reached. For the multi-step method ($n = 10$), ablation was started at 50 W. The electrical power was increased to 70 W at the fifth-step and to 90 W at the final-step. Tumor location, tumor size, and the area ablated by

Table 1. Comparison of clinical backgrounds, ablation time, and RFA-treated area size between the single-step method and the multi-step method in clinical HCC cases

	Single-step	Multi-step
n	10	10
Sex (M/F)	8/2	7/3
Age	55.6 ± 2.9	57.2 ± 2.5
Child A/Child B	8/2	9/1
Tumor location (rt./lt. lobe)	9/1	9/1
Tumor size (mm)	22.1 ± 2.1	21.1 ± 1.6
Ablation time (s)	21.4 ± 1.7	10.7 ± 2.3*
Ablated area (mm)	32.5 ± 2.4	33.6 ± 2.2

Plus–minus values are means ± SEM. Tumor size and the area ablated by RFA are expressed as the diameter (mm). χ^2-test and non-paired *t*-test showed no significant background difference between the single-step method and multi-step methods. RFA, radio frequency ablation; HCC, hepatocellular carcinoma; rt., right; lt., left; M, male; F, female. *$P<0.0001$.

RFA were determined by computed tomography examination.

Statistical analysis

All measurements were performed three times, and the results are shown as mean ± SEM. Statistical comparisons for the cumulative ablation time and the pressure at the programmed end point *in vitro* were made using ANOVA and Scheffe's test using Statview software (SAS Institute, Cary, NC, USA). Statistical comparisons for tumor size, ablation time, and the area ablated by RFA were made using non-paired *t*-test with Statview software.

Results

To determine the pressure during ablation and the time for roll-off in the single-step method, the electrode tines were expanded fully before ablation at 50 W and the pressure was measured every 20 s (Fig. 2, upper panel). In this method, the pressure increased rapidly and markedly after the ablation, it took 261.3 ± 4.67 s (mean ± SEM) to achieve roll-off and the pressure at the end point of the ablation was 837.1 ± 21.3 kPa, which is equivalent to the tire pressure of a vehicle.

In contrast to the single-step method, multi-step ablation (four- or 10-step expansion) at 50 W required a much shorter time to achieve roll-off at each step, and the pressure at the end point of the ablation also was kept very low for all steps (Fig. 2). Although the pressure at each ablation increased with the expansion of the electrode tines, the elevation of the pressure was quite gradual. Comparing four- and 10-step ablation, the latter resulted in a lower pressure and shorter time to achieve complete necrosis in the incremental steps.

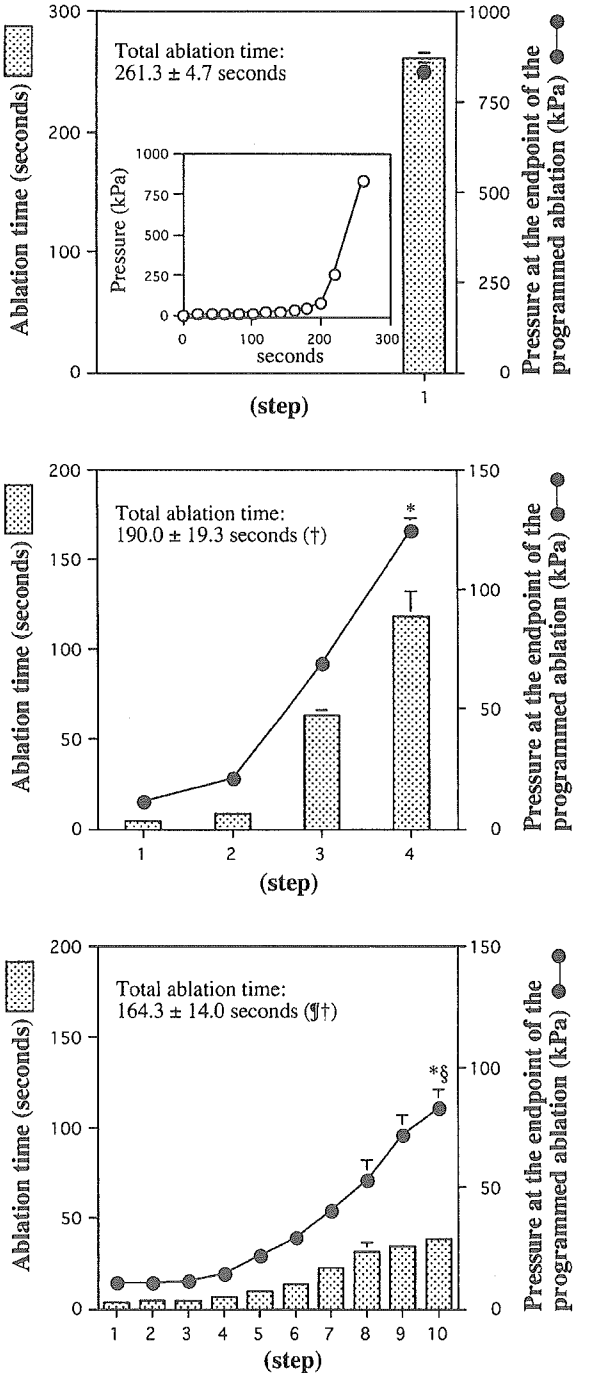

Fig. 2. The ablation time (dotted bar) and the pressure at the programmed end point (closed circle) are shown for each step. In all methods, single-step (upper panel), four-step (middle panel), and 10-step (lower panel), the ablation was performed at 50 W. The change in pressure during single-step ablation is also shown in the upper panel. The pressure was rapidly elevated after the ablation time over 200 s. The single-step method resulted in a significantly higher pressure and longer ablation time than the multi-step methods. For the multi-step methods, the 10-step ablation was shorter and finished with lower pressure than the four-step method. (*$P<0.001$ vs. single-step, §$P<0.05$ vs. four-step, †$P<0.01$ vs. single-step, ¶0.05 vs. four-step).

Comparing the cumulative ablation time of the entire process, that for the multi-step ablation was significantly shorter than that for the one-step method (Fig. 2). For the multi-step methods, the 10-step ablation time was significantly shorter than that of four-step ablation (Fig. 2).

We next evaluated the effects of the electrical power on both the time for ablation and pressure. Thirty W-ablation using the 10-step method resulted in a longer time but lower pressure to achieve roll-off in each step compared with 50 W-ablation (Fig. 3). On the other hand, 70 W-ablation using the 10-step method resulted in not only a shorter time, but also a lower pressure than 30- or 50 W-ablation (Fig. 3). Overall, 50 W-ablation resulted in the highest pressure and 30 W-ablation required the longest time to complete all steps (Fig. 3). In contrast, 70 W-ablation resulted in the lowest pressure and shortest time (Fig. 3).

Histological examination after multi-step ablation (four-step method) showed that the cell density differed between the outer and the inner portions of the ablated region (Fig. 4). That is, the cell density near the top of the needle was higher than that close to the margin of the region of ablation, whereas the difference in cell density was not seen after one-step ablation (Fig. 4).

In a preliminary clinical trial, we compared ablation time between the multi-step method ($n = 10$) and the single-step method ($n = 10$). The multi-step method showed a significantly shorter ablation time than the single-step method ($P < 0.0001$) (Table 1), and there was no significant difference in the area ablated by radio frequency. There were no adverse events during treatment with either of the methods.

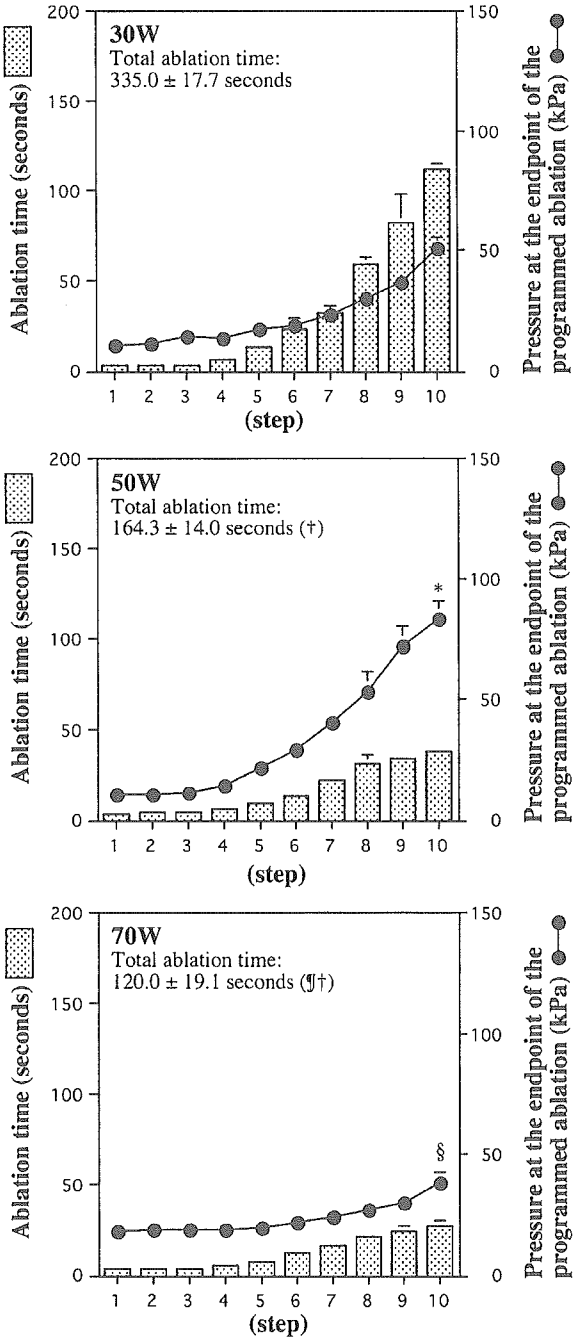

Fig. 3. The 10-step ablation was performed with varied electrical power. The ablation at 30 W took the longest, and that at 50 W resulted in the highest pressure; whereas the ablation at 70 W resulted in the shortest time and the lowest pressure. (*$P < 0.05$ vs. 30 W, §$P < 0.01$ vs. 50 W, †$P < 0.001$ vs. 30 W, ¶0.05 vs. 50 W).

Discussion

In this study, we showed that varying the setting of the RFA device could influence the ablation time and the pressure during ablation. For clinical application, we should aim for the shortest ablation time in order to reduce the patient's discomfort during treatment, and also to decrease the pressure during ablation to prevent the possibility of intra-hepatic metastasis. During RFA treatment of hepatic tumors, the pressure caused by ablation would not reach the high levels observed in this study, because the increased pressure could escape through the arteries and veins penetrating the tumor. However, a situation similar to our model could occur in a tumor with poor arterial flow and a thick capsule. The increased fibrosis in cirrhotic patients might have the same effect as a tumor capsule, containing the pressure produced by ablation.

The multi-step method required a significantly shorter ablation time and resulted in a much lower pressure during ablation than the single-step method. The difference in the ablation time is

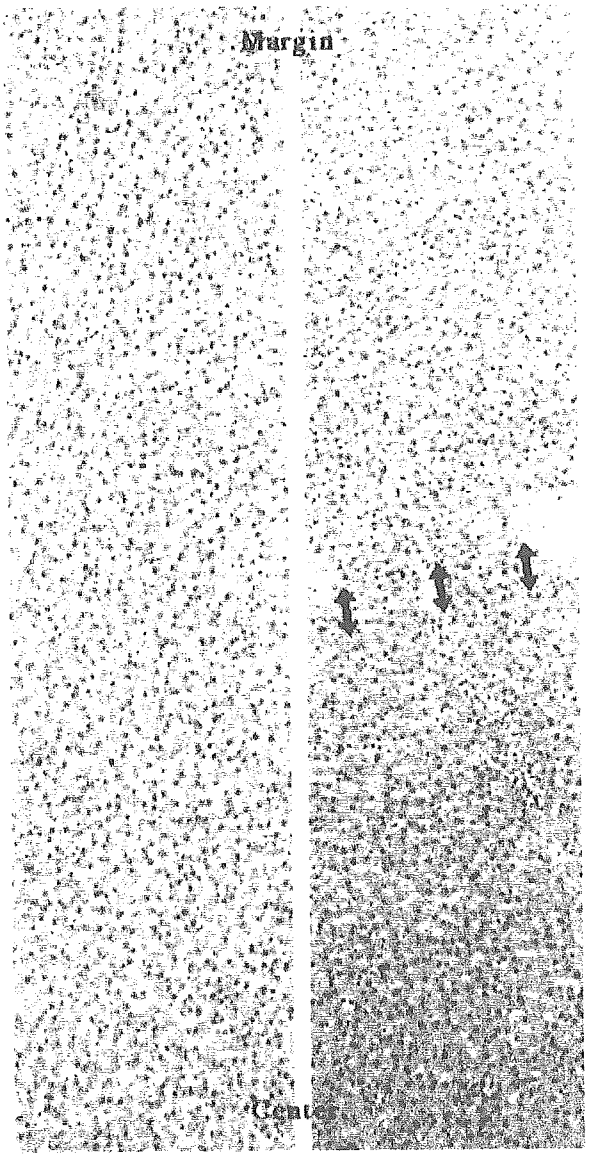

Fig. 4. Histological findings are shown after single-step (left panel) and four-step (right panel) ablation. The cell density near the center of the region of ablation was higher than that close to the margin in the four-step ablation, whereas this difference was not seen after single-step ablation. Arrows indicate the margin between the high and low cell density regions.

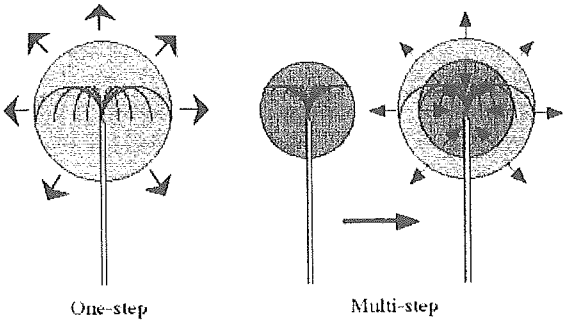

Fig. 5. A possible explanation for the mechanism of pressure reduction in the multi-step procedure, according to the histological findings in Fig. 4. Arrows indicate the pressure during RFA. In the single-step procedure, the entire ablated region is simultaneously heated, and the high pressure generated is forced outside the ablated region. In contrast, in multi-step ablation, some of the pressure caused by ablation during the second and subsequent steps could escape into the internal region, resulting in lower pressure than in the single-step ablation.

thought to be attributable to the efficiency of energy use. That is, the single-step procedure requires continuous ablation until the entire targeted region becomes necrotic. Furthermore, the extra-tumorous tissue, in addition to the tumor, is heated, resulting in wasted energy. In contrast, in the multi-step procedure, the region of ablation is limited in each step, preventing unnecessary energy loss.

That difference in the region of ablation may also explain the inequality in pressure during ablation. In the single-step procedure, all ablated cells in the entire targeted region would expand simultaneously to generate high pressure, while the ablation of a limited region in the multi-step procedure would result in a lower level of intra-tumor pressure. Furthermore, histological findings indicated another mechanism of pressure reduction in the multi-step procedure. After multi-step ablation, the cell density of the internal region was higher than that of the outer region. We speculate that this indicates that some of the pressure caused by ablation during the second and subsequent steps could escape into the internal region, which was ablated in previous steps, and the cells within it would become friable (Fig. 5).

Considering the mechanism of the successive effects during the multi-step procedures, it is inevitable that the 10-step procedure is superior to the four-step, because the greater the number of steps used for ablation, the lower the pressure and the shorter the time required. Because the procedure becomes increasingly complicated as more steps are added, we propose that an eight- to 10-step procedure is efficient and effective in clinical application.

The electrical power used for RFA is another parameter that should be carefully considered. According to the manual of the device, it is recommended that ablation should be started at 50 W and the electrical power should be increased by 10 W/min in the subsequent ablation until 90 W is reached. The reason the ablation is started at low power is essentially to decrease the pain of the patient. However, the relationship between the electrical power and the intra-tumor pressure, and the duration of the ablation, has not been clarified. Our results showed that the

ablation time became shorter with the increase in the electrical power, whereas the intra-tissue pressure increased at 50 W but subsequently decreased at 70 W (Fig. 3). The inverse relationship between the duration and the electrical power is easily understood, but the decreased pressure at high power seems paradoxical. One possible explanation of this paradox is that the ablation with very high electrical power may achieve complete necrosis rapidly, before the tissue temperature around the targeted region increases, so that the total pressure would be kept at a relatively low level. If we accept this explanation, the ablation time could be shortened and the intra-tumor pressure would decrease with an increase in the electrical power, without limitation. But we must remember that ablation at high power induces severe pain. Therefore, the upper limit of the electrical power should be determined according to the suffering of the patient and the extent of the pressure reduction. We are now applying our multi-step method in clinical RFA treatment, and preliminary results indicate that the multi-step method had significantly shorter ablation times than the single-step method (Table 1). We plan to further evaluate the appropriateness of this procedure for clinical use, and confirm whether the intra-tumor pressure created by the sudden heating of RFA contributes to the spreading or local recurrence of HCC.

In this study, we showed that the standard, single-step method might entail a risk of extreme increases in intra-tumor pressure under some conditions, which could result in scattering of intra-hepatic metastasis. Our model is artificial and without blood flow, and a system with perfusion using an entire liver would be required to simulate the condition of a living liver more accurately. Finally, we emphasize that intra-tumor pressure could be greatly reduced by a simple modification of the use of the standard device, simply by adopting an incremental, multi-step method. We believe that this multi-step method should be applied as a standard clinical procedure for RFA.

References

1. Ohishi W, Kitamoto M, Aikata H, Kamada K, Kawakami Y, Ishihara H, Kamiyasu M, et al. Impact of aging on the development of hepatocellular carcinoma in patients with hepatitis C virus infection in Japan. Scand J Gastroenterol 2003; 38: 894–900.
2. Ichida T, Van Thiel D H, Hassanein T. The medical management of hepatocellular carcinoma (HCC) in Japan: a review with implications for HCC seen in the west. Hepatogastroenterology 1996; 43: 1575–83.
3. Kotoh K, Sakai H, Sakamoto S, Nakayama S, Satoh M, Morotomi I, Nawata H. The effect of percutaneous ethanol injection therapy on small solitary hepatocellular carcinoma is comparable to that of hepatectomy. Am J Gastroenterol 1994; 89: 194–8.
4. Kotoh K, Sakai H, Morotomi I, Nawata H. The use of percutaneous ethanol injection therapy for recurrence of hepatocellular carcinoma. Hepatogastroenterology 1995; 42: 197–200.
5. Yamamoto J, Okada S, Shimada K, Okusaka T, Yamasaki S, Ueno H, Kosuge T. Treatment strategy for small hepatocellular carcinoma: comparison of long-term results after percutaneous ethanol injection therapy and surgical resection. Hepatology 2001; 34: 707–13.
6. Buscarini L, Buscarini E, Di Stasi M, Vallisa D, Quaretti P, Rocca A. Percutaneous radiofrequency ablation of small hepatocellular carcinoma: long-term results. Eur Radiol 2001; 11: 914–21.
7. Giovannini M, Moutardier V, Danisi C, Bories E, Pesenti C, Delpero J R. Treatment of hepatocellular carcinoma using percutaneous radiofrequency thermoablation: results and outcomes in 56 patients. J Gastrointest Surg 2003; 7: 791–6.
8. Llovet J M, Vilana R, Bru C, Bianchi L, Salmeron J M, Boix L, Ganau S, et al. Increased risk of tumor seeding after percutaneous radiofrequency ablation for single hepatocellular carcinoma. Hepatology 2001; 33: 1124–9.
9. Horiike N, Iuchi H, Ninomiya T, Kawai K, Kumagi T, Michitaka K, Masumoto T, et al. Influencing factors for recurrence of hepatocellular carcinoma treated with radiofrequency ablation. Oncol Rep 2002; 9: 1059–62.
10. Catalano O, Lobianco R, Esposito M, Siani A. Hepatocellular carcinoma recurrence after percutaneous ablation therapy: helical CT patterns. Abdom Imaging 2001; 26: 375–83.
11. Chopra S, Dodd G D 3rd, Chintapalli K N, Leyendecker J R, Karahan O I, Rhim H. Tumor recurrence after radiofrequency thermal ablation of hepatic tumors: spectrum of findings on dual-phase contrast-enhanced CT. Am J Roentgenol 2001; 177: 381–7.
12. Harrison L E, Koneru B, Baramipour P, Fisher A, Barone A, Wilson D, Dela Torre A, et al. Locoregional recurrences are frequent after radiofrequency ablation for hepatocellular carcinoma. J Am Coll Surg 2003; 197: 759–64.
13. Takada Y, Kurata M, Ohkohchi N. Rapid and aggressive recurrence accompanied by portal tumor thrombus after radiofrequency ablation for hepatocellular carcinoma. Int J Clin Oncol 2003; 8: 332–5.
14. Koda M, Maeda Y, Matsunaga Y, Mimura K, Murawaki Y, Horie Y. Hepatocellular carcinoma with sarcomatous change arising after radiofrequency ablation for well-differentiated hepatocellular carcinoma. Hepatol Res 2003; 27: 163–7.

Human Pathology (2005) 36, 878–885

ELSEVIER

Human PATHOLOGY

www.elsevier.com/locate/humpath

Splenic large B-cell lymphoma in patients with hepatitis C virus infection☆

Morishige Takeshita MD[a,*], Hironori Sakai MD[b], Seiichi Okamura MD[b], Yumi Oshiro MD[c], Koichi Higaki MD[d], Osamu Nakashima MD[e], Naokuni Uike MD[f], Ichiro Yamamoto MD[g], Mitsuru Kinjo MD[h], Fujio Matsubara MD[i]

[a]*Department of Pathology, School of Medicine, Fukuoka University, Fukuoka 814-0180, Japan*
[b]*Clinical Research Institute, National Kyushu Medical Center, Fukuoka, Japan*
[c]*Department of Pathology, Matsuyama Red-Cross Hospital, Ehime, Japan*
[d]*Department of Pathology, Saint Mary Hospital, Kurume, Japan*
[e]*Department of Pathology, School of Medicine, Kurume University, Kurume, Japan*
[f]*Department of Hematology, National Kyushu Cancer Center, Fukuoka, Japan*
[g]*Department of Pathology, Hamanomachi Hospital, Fukuoka, Japan*
[h]*Department of Pathology, Nippon Steel/Yahata Memorial Hospital, Kitakyushu, Japan*
[i]*Department of Internal Medicine, Shin-Kokura Hospital, Kitakyushu, Japan*

Received 18 January 2005; accepted 1 June 2005

Keywords:
HCV;
HBV;
Spleen;
Malignant lymphoma

Summary Hepatitis virus infection, especially type C (hepatitis C virus [HCV]), has been suggested to be one of the important pathogenetic factors for low- and high-grade B-cell lymphoma, including splenic marginal zone lymphoma (SMZL), in southern Europe. Here, we analyzed the incidences of HCV and hepatitis B virus (HBV) infections, and the clinicopathologic features in 29 cases of splenic diffuse large B-cell lymphoma (DLBCL), 10 SMZL, 3 splenic mantle cell lymphoma, 1 hairy cell leukemia, 13 B-chronic lymphocytic leukemia, and 12 hepatosplenic T-cell and natural killer cell lymphoma. Fifteen (51.7%) splenic DLBCL cases were HCV antibody–positive, and another 6 (20.7%) had the HBsAg. The incidence of each was significantly ($P < .01$) higher than those of HCV (9.3%) and HBV (1.9%) infections in 54 node-based DLBCL cases. Four examined HCV-positive DLBCL cases showed no type II cryoglobulinemia. HCV RNA was detected in fresh tumor tissues from 6 of 7 examined DLBCL cases, and HBV DNA was present in another 2, as evaluated by real-time polymerase chain reaction. Immunohistologically, tumor cells in 5 of 7 examined DLBCL cases showed intracytoplasmic reactions for HCV NS3 and E2 proteins and the viral receptor CD81. Of 6 cases, 2 showed an intranuclear reaction for the HBV surface protein. By Southern blot analysis, no rearrangement of the *Bcl2* gene was detected in the tumor tissue of 7 HCV-positive DLBCL cases. For the other types of malignant lymphoma, 1 case each of SMZL (10%) and hepatosplenic T-cell and

☆ This study was supported in part by Health and Labour Sciences Research Grants on Hepatitis, Tokyo, Japan.
* Corresponding author. Department of Pathology, School of Medicine, Fukuoka University, Nanakuma 7-45-1, Johnan-ku, Fukuoka 814-0180, Japan.
E-mail address: m-take@fukuoka-u.ac.jp (M. Takeshita).

0046-8177/$ – see front matter
doi:10.1016/j.humpath.2005.06.005

natural killer cell lymphoma (8.3%) showed HCV infection. In conclusion, persistent human hepatitis virus infections, especially HCV, may play an important role in the tumorigenesis of splenic DLBCL in Japan.

1. Introduction

Hepatitis C virus (HCV) infection may be involved in the pathogenesis of type II (monoclonal IgM and polyclonal IgG) cryoglobulinemia (CG) and low- and high-grade B-cell malignant lymphoma (ML) in southern Europe [1,2]. De Vita et al [3] reported that B-cell ML in HCV-positive patients presented extranodal localization frequently in the bone marrow and major salivary glands and occasionally in the liver and spleen and histologically showed lymphoplasmacytic lymphoma (LPL) and diffuse large B-cell lymphoma (DLBCL). Serology of HCV infection was found in 11 (35%) of 31 Italian cases of splenic marginal zone lymphoma (SMZL) [4]. Hermine et al [5] further reported 9 French cases of HCV-positive SMZL with type II CG. Because these 9 cases showed loss of HCV RNA in their sera and complete remission of ML after interferon (IFN) α and ribavirin treatments, the authors suggested that HCV infection plays a role in the lymphomagenesis of SMZL. Japan is also an endemic area for HCV infection, and HCV-related ML cases have been reported [6,7]. Although SMZL is rare among the total ML cases in Japan [8], we examined the relationships between the histological types of spleen-involving ML and hepatitis virus (HV) infection. We found a high incidence of HCV infection in splenic DLBCL cases and a low incidence in SMZL. We discuss the cause of the strikingly different histological types of splenic B-cell ML with HCV infection between Japanese and southern European patients. Sansonno et al [9] demonstrated HCV RNA in reactive lymph nodes and neoplastic tumor tissues of B-cell ML by reverse transcription–polymerase chain reaction (PCR) and immunohistologically detected the HCV core and NS3- and NS4-related proteins, C100, c22, and c33, in the tumor tissues of 3 of 12 HCV-positive B-cell ML cases. The HCV-encoded NS3 protease and helicase have central roles in the viral replication cycle [10]. The E2 protein of HCV binds the CD81 receptor in B lymphocytes, and internalization of the virus may activate the signaling pathway and induce lymphomagenesis [11]. We found the presence of HCV RNA in the tumor tissues of ML by real-time PCR and also detected HCV NS3 and E2 proteins plus CD81 in the lymphoma cells. The etiologic role of HCV infection is discussed.

It is known that *Bcl2* is an important apoptosis inhibitor for B cells and their neoplasm and that *Bcl2* translocation is frequently detected by PCR in the peripheral blood mononuclear cells (PBMCs) of patients with HCV infection [12]. *Bcl2* gene expression may reflect a premalignant state of B cells with HCV infection. We examined for any rearrangements of the *Bcl2* and *Bcl6* genes and proteins in the tumor tissues.

Hepatitis B virus (HBV) may also play an important role in lymphomagenesis in B-cell ML [13]. The influence of HBV infection in splenic ML is discussed.

2. Patients and methods

We investigated 68 patients with ML, primarily involving the spleen. Thirteen cases of B-chronic lymphocytic leukemia (CLL) and 12 of hepatosplenic T-cell lymphoma and aggressive natural killer (NK) cell leukemia/lymphoma (HST/NKL), which mainly involved the spleen, were included. The clinical and laboratory findings, treatments, and prognoses were examined for each hospital. Fifty-four node-based DLBCL cases and 445 colon cancer cases admitted to the National Kyushu Medical Center were selected for examination of their HCV and HBV infections as a control. Precipitated serum cryoglobulin was measured using a micro–TP-AR kit (Wako Chemical Industries, Osaka, Japan), and the immunoglobulin composition was determined by immunoelectrophoresis.

2.1. Examination of HCV and HBV infections

Serum samples were screened for HCV infection by assaying the amount of anti-HCV antibodies using a second-generation enzyme-linked immunosorbent assay technique. The HCV genotype was determined by a PCR-based technique (SMI Test HCV Genotyping Kit; Sumitomo Metals, Osaka, Japan), which identified 4 genotypes (1a, 1b, 2a, and 2b) according to the classification of Simmonds et al [14]. HBV surface and envelope antigens were also screened with an enzyme-linked immunosorbent assay kit (Abbott Laboratories, Abbott Park, Ill).

2.2. Quantitative real-time PCR for HCV RNA and HBV DNA

Fresh frozen tumor tissues of 8 HCV-positive splenic ML cases and reactive lymph nodes of 3 HCV-positive cases were examined. Total RNA was extracted from 10-mg fresh frozen tumor tissues from HCV-positive ML patients using the isogen-LS RNA extraction system (Nipon Gene, Tokyo, Japan). Purified RNA was suspended in 20 μL of diethyl pyrocarbonate–treated water containing 10 mmol/L dithiothreitol and 200 U/mL ribonuclease inhibitor. The RNA

Table 1 Antibodies used in immunostaining and detection kit

Antibody	Clone	CD no.	Source
CD3	PS1	CD3ε	Novocastra
CD5	4C7	CD5	Novocastra
CD10	56C6	CD10	Novocastra
CD20	L26	CD20cy	Dako
IL-2 receptor	4C9	CD25	Novocastra
CD103	2G5	CD103	Immunotech
Bcl1	5D4		IBL
Bcl2	124		Dako
Bcl6	P1F6		Novocastra
NCAM1	123C3.D5	CD56	NeoMarkers
TIA1	NS/1-AG4		Coulter
CD81	1D6	CD81	Novocastra
HCV NS3	MMM33		Novocastra
HCV E2			ViroStat
HBs Ag	ZCH16		Nichirei
HHV-8 LNA	13B10		Novocastra
In situ hybridization and detection kit for EBER (Rembrandt)			Kreateck

TIA1, T-cell intercellular antigen; LNA, latent nuclear antigen. Company locations are as follows: Novocastra, Newcastle upon Tyne, England; Dako, Carpinteria, CA; Immunotech, Marseille, France; IBL, Takasaki, Japan; Neomakers, Fremont, CA; Coulter, Hialeah, FL; ViroStat, Portland, ME; Nichirei, Tokyo, Japan; Kreateck, Amsterdam, Netherlands.

solution was used for real-time PCR, which was performed using a TaqMan EZ RT-PCR Core Reagent kit and an ABI 7700 sequence detector system (Perkin Elmer, Foster City, Calif) [15]. HBV DNA was extracted from 10-mg fresh frozen tumor tissues and was determined by real-time PCR as described previously [16].

2.3. Histology, immunohistology, and in situ hybridization

Tissue specimens were fixed with 20% formalin, embedded in paraffin, and stained with hematoxylin-eosin solution. The histological diagnosis of the first biopsy and resected samples and the primary sites were decided according to the World Health Organization classification and its criteria [17]. For immunohistology, a battery of monoclonal antibodies (Table 1) was applied to formalin-fixed samples using the Chemmate Envision method (Dako, Carpinteria, Calif) and an alkaline phosphatase–conjugated avidin-biotin method (Vector, Burlingame, Calif). Human herpesvirus (HHV) 8 infection was checked by immunohistology for the HHV-8–encoded protein latent nuclear antigen (LNA). To detect Epstein-Barr virus (EBV) infection, paraffin sections were hybridized in a solution of 50% formamide-containing digoxigenin/biotin-labeled EBV-encoded RNA (EBER) oligonucleotides (Rembrandt Kit, Kreateck, Amsterdam, The Netherlands).

2.4. Detection of the Bcl2 and Bcl6 genes

Fresh frozen tumor tissues from 8 HCV-positive B-cell ML cases and reactive lymph nodes of 2 HCV-positive cases were examined. Rearrangements of the *Bcl2* and *Bcl6* genes were analyzed using *Bcl2* MRB and mcr probes, and *Bcl6* LAZ3-A and LAZ3-2 probes, respectively. Five-microgram aliquots of genomic DNA were digested with *Bam*HI or *Hin*dIII restriction endonucleases, electrophoresed in 0.8% or 1% agarose gels, denatured with alkali, neutralized, and then transferred to nitrocellulose filters. The filters were hybridized in 50% formamide/3× standard citrate buffer at 37°C with DNA probes that had been labeled with phosphorus 32 using a Random Primed DNA labeling kit (Boehringer Mannheim, Mannheim, Germany).

2.5. Statistical analyses

To confirm differences between 2 groups of lymphoma patients, univariate analyses by the χ^2 and Fisher tests were performed.

Table 2 Clinical findings of ML, mainly involving spleen

	Diffuse large B-cell ML	Marginal zone	Mantle cell ML	B-CLL	Hepatosplenic T-/NK cell ML
No. of cases	29	10	3	13	12
Median age (y)	64.6	64	76	64	54
Sex (M/F)	22:7	7:3	1:2	9:4	7:5
Positive HCV antibody	15	1	0	0	1
Positive HBsAg	6	2	0	1	0
CH/LC/HCC	17:3:1	3:0:0	0	1:0:0	1:0:0
Clinical stage					
I, II	22	4	0	0	0
III, IV	7	6	3	13	12
Splenectomy	25	9	3	0	0
Mean weight of spleen (g)	560	1610	1980	NT	560 at autopsy
Macroscopic feature					
Nodular tumors	29	0	0	0	0
Diffuse infiltration	0	10	3	13	12

Abbreviations. M, male; F, female; CH, chronic hepatitis; LC, liver cirrhosis; HCC, hepatocellular carcinoma; NT, not tested.

3. Results

3.1. Clinical findings, laboratory data, treatment, and outcome

Clinicopathologically, we classified 29 cases of DLBCL, 10 of SMZL, 3 of CD5-positive mantle cell lymphoma, 1 of hairy cell leukemia, 13 of B-CLL, and 12 of HST/NKL. The clinical data of the 5 ML groups, except for the hairy cell leukemia case, are detailed in Table 2.

3.2. Splenic DLBCL

The median age at diagnosis was 64.6 years (range, 37-83 years). Fifteen (51.7%) splenic DLBCL cases showed serum HCV antibodies, and this prevalence was significantly ($P < .01$) higher than the 5 (9.3%) of 54 nodal DLBCL and 23 (5.2%) of 445 colon cancer cases. Another 6 (20.7%) cases had HBsAg and/or HBeAg, and this prevalence was also significantly ($P < .01$) higher than the 1 (1.9%) of 54 nodal DLBCL cases and 7 (1.6%) of 445 colon cancer cases. Three of the examined HCV-positive cases showed the 1b genotype in their sera and another case was 2b. No type II CG was detected in the 4 examined cases. Twelve cases had a history of chronic hepatitis and 3 had liver cirrhosis, whereas the remaining 6 were healthy carriers. By computed tomography, splenomegaly and large nodular tumors were detected in all the cases. Twenty-five cases received a splenectomy (Fig. 1A), and the mean weight of the removed spleen in these cases was 560 g. In another 4 cases, histological diagnosis was performed using the involved lymph nodes and the liver. Twenty-two cases were classified as stage I or II. Eight cases received a splenectomy, and no further treatments were performed. Combination chemotherapy was performed in 8 cases, and splenic radiation and combination chemotherapy were performed in 7. Six cases were not followed. Eighteen cases showed complete and partial remission from 8 to 84 months. Another 5 cases died, and among these, 4 died of liver dysfunction due to cirrhosis or hepatocellular carcinoma. The 5-year survival of HCV-positive cases was

Table 3 Immunohistological findings and EBV infection of ML

	Diffuse large B-cell	Marginal zone	Mantle cell ML	B-CLL	Hepatosplenic T-/NK cell ML
No. of cases	29	10	3	13	12
CD5	0	0	3	10/12	NT
CD10	6	0	0	0	0
CD20	29	8	3	13	0
Bcl1	0	0	2	0/12	NT
Bcl2	11/24	5	2	12/12	NT
Bcl6	15/24	0	0	0/12	NT
CD25	9/24	0	1/3	7/12	NT
CD3	0	0	0	0	8
TIA1	NT	NT	NT	NT	9/11
CD56	NT	NT	NT	NT	5
HHV-8 LNA	0/24	0/6	0	NT	NT
EBERs (ISH)	1/24	0/6	0	0	5/10

NOTE. Fractions are positive cases/examined cases. Abbreviation. ISH, in situ hybridization.

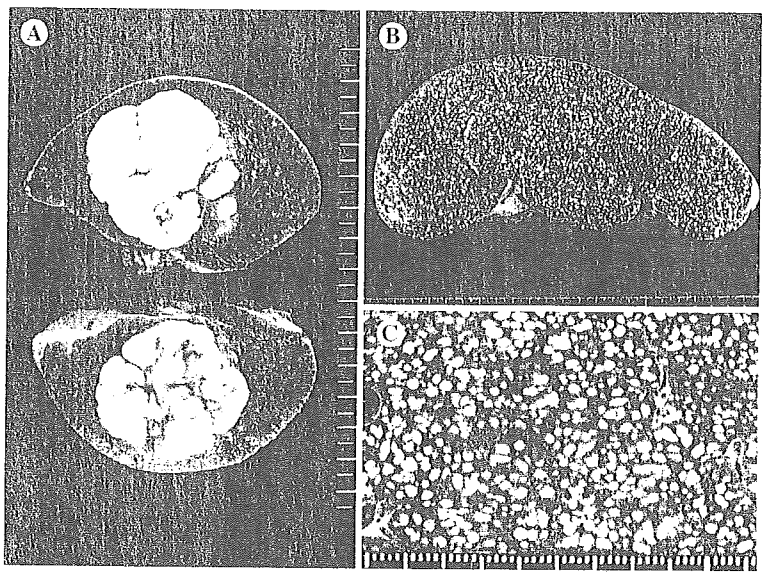

Fig. 1 A, Macroscopic findings of splenic DLBCL with HCV infection. A large lobulated tumor is detected in the spleen. B and C, Macroscopic findings of SMZL without HCV infection. Many small miliary nodules are detected.

Table 4 Relationship among clinicopathologic findings, HCV infection, and *Bcl* genes of frozen tumor tissues

	Age (y)	Sex	CG	Serum HCV		Hepatic disorder	Primary tumor site	Histology	HCV RNA copy per 10 mg	Immunohistology			Rearrangement of *Bcl* genes		Immunohistology		
				Ab	Genotype					HCV NS3	HCV E2	CD81	*Bcl2*	*Bcl6*	CD10	Bcl2	Bcl6
1	60	M	–	+	1b	CH	Spleen	DLBCL	4.1×10^2	+	+	+	–	–	–	–	+
2	59	M	–	+	1b	CH	Spleen	DLBCL	2.5×10^2	+	+	+	–	–	–	+	+
3	69	M	–	+	2b	CH	Spleen	DLBCL	1.9×10^5	+	+	+	–	+	–	–	+
4	59	F	NT	+	NT	CH	Spleen	DLBCL	4.0×10^5	+	+	+	–	–	–	+	–
5	49	M	NT	+	1b	CH	Spleen	DLBCL	5.5×10^4	–*	–*	+	–	–	–	+	+
6	53	F	NT	+	NT	CH	Spleen	DLBCL	1.4×10^3	+	+	+	–	+	+	–	+
7	67	M	NT	+	NT	CH	Spleen	DLBCL	0	–	–	+	–	–	–	–	+
8	71	F	NT	+	1b	CH	Spleen	Marginal	0	–	–	+	–	–	–	+	–
C1	69	F	–	+	1b	CH	LN	Reactive	9.5×10^3	–*	–*	–**	–	+	R+	R+	R+
C2	61	M	–	+	1b	CH	LN	Reactive	2.9×10^2	NT	NT	NT	–	–	R+	R+	R+
C3	74	M	–	+	1b	CH	LN	Reactive	8.0×10^4	NT	NT	NT	NT	NT	R+	R+	R+

Abbreviations. Ab, antibody; M, male; F, female; LN, lymph node; R, reactive changes.
* HCV NS3– or E2-positive small lymphocytes are found.
** CD81-positive histiocytes are present.

86% by the Kaplan-Meier method, and that of HV-negative cases was 100%.

3.3. Immunohistological findings and EBV infection in splenic DLBCL

Immunohistologically, 6 (31%) of 29 DLBCL cases showed a positive reaction for CD10, and 9 (37.5%) of 24 were positive for CD25. *Bcl6*-positive lymphoma cells were found in 16 (66.7%) of 24 cases, and *Bcl2* was found in 11 (45.8%). No positive reaction for HHV-8 LNA was detected in any of the 24 examined DLBCL cases. By in situ hybridization, only 1 of 24 examined DLBCL cases possessed EBER-positive tumor cells (Table 3).

3.4. Other types of lymphoma primarily involving the spleen

One of the 10 SMZL cases showed HCV infection, and 2 others showed HBV infection. Nine cases received a

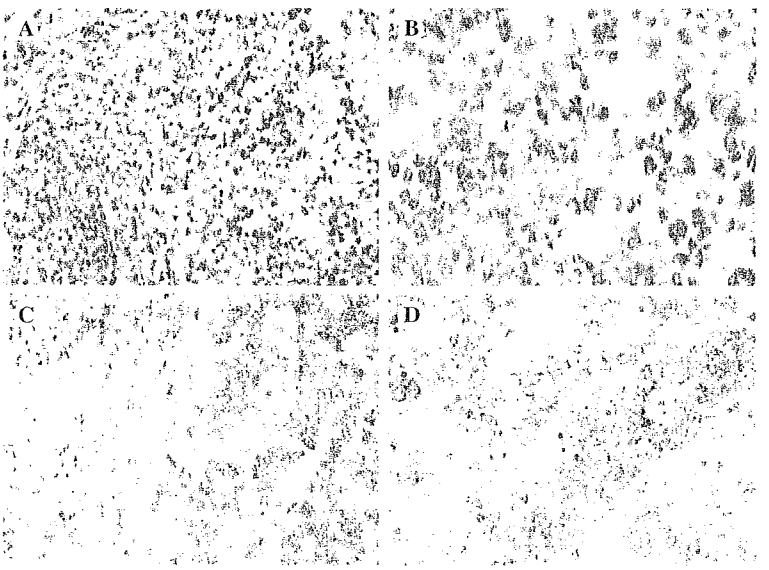

Fig. 2 A, Immunohistology of HCV NS3 protein in the spleen. Some scattered reactive lymphocytes are detected in the red pulp outside the DLBCL (avidin-biotin complex method, original magnification ×200). B, A high-magnification image of HCV NS3–positive reactive lymphocytes (original magnification ×400). C, Immunohistology of HCV NS3 protein in DLBCL. Large tumor cells show an intracytoplasmic reaction for HCV NS3 protein (original magnification ×300). D, Immunohistology of the HCV E2 protein in DLBCL. Many tumor cells are positive for the HCV E2 protein (original magnification ×400).

splenectomy, and the mean weight of the removed spleen in these cases was 1610 g, which was significantly ($P < .01$) heavier than that of the DLBCL cases. Numerous white miliary nodules were detected in the whole spleens, and no large tumor formations were detected (Fig. 1B and C). Six cases were classified as stage III or IV, and combined chemotherapy was performed in 10 cases. Only 1 case without HV infection died of disease at 34 months. Three cases of splenic mantle cell lymphoma had no HV infection. Among 13 cases of B-CLL, 1 case was positive for the HBsAg and HBeAg. One case of CD25- and CD103-positive hairy cell leukemia was HBsAg- and HCV antibody–negative. In 12 HST/NKL cases, only 1 aggressive NKL was HCV antibody–positive.

3.5. Detection of HCV RNA, HBV DNA, and HV antigens

The detailed findings for tissue HCV RNA and immunohistology of HCV antigens are shown in Table 4. Of 7 DLBCL cases with the HCV antibody in their sera, 6 showed between 1.4×10^3 and 4.0×10^4 copies of HCV RNA per 10-mg tumor tissues by real-time PCR. In 1 SMZL case showing the HCV 1b genotype in the serum, HCV RNA was not detected in the involved tissue. HCV RNA was detected in the reactive lymph nodes of 3 HCV-positive cases. Immunohistologically, weak positive reactions for the HCV NS3 and E2 proteins were detected in the cytoplasm of many lymphoma cells in 5 of 7 DLBCL cases (Fig. 2) but not in 1 SMZL case. Outside the tumors, some HCV NS3– and E2 protein–positive reactive lymphocytes were detected, mainly in the marginal zone and red pulp (Fig. 2). Lymphoma cells and scattered histiocytes were positive for CD81 in 7 DLBCL cases. Among these cases, the lymphoma cells in 2 HCV protein–negative cases showed a positive reaction for CD81. Two examined DLBCL cases showed 1.8×10^3 and 1.6×10^4 copies of HBV DNA per 10-mg tumor tissues by real-time PCR. Immunohistologically, the large lymphoma cells in 2 of 6 DLBCL cases showed a weak nuclear reaction for the HBs protein in the formalin-fixed tumor tissues.

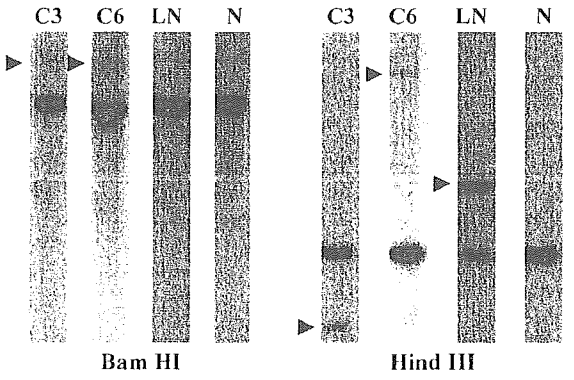

Fig. 3 Southern blot analysis of *Bcl6* genes. Genomic DNAs of fresh frozen tissues are digested with *Bam*HI or *Hin*dIII. Cases 3 and 6 of HCV-positive splenic DLBCL and a control case of HCV-positive reactive lymph node show rearrangements of *Bcl6* genes. Genomic DNA of a HCV-negative reactive tonsil is used as a negative control. NOTE. Arrowheads indicate rearranged bands. Abbreviations. C3, case 3; C6, case 6; LN, control case of HCV-positive reactive lymph node; N, negative control.

3.6. Examination of the Bcl2 and Bcl6 genes and proteins

These data are also shown in Table 4. No rearrangement of the *Bcl2* gene was detected in the fresh tumor tissues of 7 DLBCL cases, whereas 2 DLBCL cases and 1 reactive lymph node showed rearrangement of the *Bcl6* gene (Fig. 3). Immunohistologically, 3 of 7 DLBCL cases showed a positive reaction for the *Bcl2* protein and 6 were positive for *Bcl6*.

4. Discussion

Saadoun et al [18] demonstrated that treatment with IFN alone or a combination of IFN and ribavirin led to a complete virologic response and hematologic remission as well as the disappearance of type II CG and its clinical symptoms in 16 of 18 examined HCV-positive SMZL cases. The monoclonal IgM of type II CG, which is frequently (17.3%) found in HCV-positive patients [19], is mostly encoded by a restricted set of immunoglobulin V region genes, *VH1-69* and *Vκ3-A27*, which are also expressed in more than half the cases of HCV-positive LPL and salivary gland MALToma [20,21]. It has been suggested that HCV-positive type II CG is a prodromal phase in cases of SMZL, LPL of the bone marrow, and salivary gland MALToma in southern Europe. The HCV prevalence (2.5%) in blood donors of 50 to 64 years in Japan was similar to that (2.4%) in blood donors older than 40 years in Italy [22], and the HCV genotypes did not differ between Japanese and Italian cases of B-cell ML [3,23]. However, the incidence of type II CG is 1.5% in HCV-positive Japanese cases [24] and 3.5% in HCV-positive B-cell ML [23]. In this study, only 1 (10%) SMZL case had HCV infection, and 4 HCV-positive DLBCL cases and 3 HCV-positive reactive lymphadenitis cases examined had no type II CG. It is strongly speculated that the rare incidence of type II CG and its low association with abnormal B-cell proliferation in HCV-positive cases influence the low incidence of SMZL. Lenzi et al [25] demonstrated that haplotype HLA-B8-DR3 may be considered as a risk factor for developing HCV-positive CG in Italy. However, the haplotype was not found in Japanese HCV-positive cases either with or without CG [26]. Therefore, host genetic factors may influence the incidence of type II CG in HCV-positive cases.

On the other hand, the prevalence (51.7%) of HCV infection in the examined splenic DLBCL cases was significantly ($P < .05$) higher than those in the SMZL and node-based DLBCL cases. Some HCV-positive splenic

DLBCL cases have been reported [3,7], but no detailed analyses of the relationship between splenic DLBCL and HCV infection have been performed. Murakami et al [27] found a high prevalence (14.3%) of chronic liver disease in 98 reported Japanese cases of splenic ML in 1988. Although no adequate virologic examination was performed, they speculated that chronic liver disease has some etiologic influence on splenic ML. Among 15 examined splenic DLBCL cases with HCV infection, 12 had chronic hepatitis or were healthy carriers. HCV infection, which is independent of the degree of hepatic dysfunction, may influence the local immune system and play a role in the lymphomagenesis of splenic DLBCL.

De Vita et al [3] demonstrated that type II CG was only detected in 4 (17.4%) of 23 HCV-positive DLBCL cases and suggested that HCV-positive B-cell ML without type II CG tends to show high-grade B-cell ML [3,28]. Our 4 examined HCV-positive splenic DLBCL cases did not show type II CG. However, 3 of 4 HCV-positive hepatic DLBCL cases were reported to have type II CG in France [29]. Further studies are necessary to examine which kinds of factors influence the occurrence of HCV-positive splenic DLBCL.

Using reverse transcription PCR, Luppi et al [30] detected HCV RNA in tumor tissues from 6 of 8 low-grade MALToma cases, 5 of 8 follicular lymphoma, and only 1 of 14 Hodgkin lymphoma but not in tumor tissues from 10 T-cell lymphoma cases. Immunohistologically, the HCV core and NS3 and NS4 proteins C100, c22, and c33 were mainly detected in lymphocytes in the interfollicular area of reactive lymph nodes and in 3 follicular lymphoma cases among 12 HCV-positive B-cell ML [9]. We also found HCV RNA in tumor tissues from 6 of 7 examined splenic DLBCL cases as well as from 3 reactive lymph node cases by real-time PCR. Furthermore, the HCV NS3 and E2 proteins were detected in the lymphoma cells of 5 of 7 DLBCL cases. It was previously reported that NS3 was able to transform a nonneoplastic mouse fibroblastic cell line into a fibrosarcoma [31]. Hofmann et al [32] demonstrated that the HCV E2 protein may induce B-cell proliferation in vitro and the development of type II CG in vivo. HCV may replicate in B cells and be closely connected with B-cell lymphoma in HCV-positive patients.

CD81 has been identified as a receptor for the HCV E2 protein in B cells [11]. In the current study, CD81 was positive in the lymphoma cells of 7 HCV-positive splenic DLBCL cases and even in those of the 2 HCV E2 protein–negative cases. CD81, which belongs to the tetraspanin family, also has close associations with major histocompatibility complex class I and II proteins [33]. It was also detected in 19 of 21 Burkitt cell lines, which are not connected with HCV infection [34]. Therefore, CD81 may play a role not only as a receptor for HCV E2 protein but also in signaling through major histocompatibility complex molecules in B cells.

Sasso et al [35] reported a high joining rate (82%) of the *Bcl2* gene to immunoglobulin J_H6 in the PBMCs of HCV-positive cases by nucleotide sequence analysis, which was significantly ($P = .03$) higher than the rate for normal controls (38%) and similar to that (66%) of HCV-positive B-cell ML cases. However, Boiocchi [36] demonstrated that *Bcl2* translocation occurred in PBMCs from ML cases independently of HCV infection, and only 4 (12.5%) of 32 cases showed rearrangement of the *Bcl2* gene in the tumor tissue of HCV-positive B-cell ML. These authors suggested that the *Bcl2* gene is not the main inducer of lymphomagenesis in HCV-positive B-cell ML. In our study, 7 splenic DLBCL cases with HCV infection showed no rearrangement of the *Bcl2* gene in their tumor tissues by Southern blot analysis, and only 2 had a rearrangement of the *Bcl6* gene. Mutations of the *V*H and *Bcl6* genes as well as the p53 and β-catenin genes occurred 7-fold more frequently in HCV-positive B-cell lines and ML cases than in HCV-negative controls [37]. Different kinds of mutations in the cell cycle and apoptotic pathway may be required for HCV-positive, low- and high-grade B-cell ML.

Stoll-Becker et al [38] detected different HBV messenger RNA transcripts in PBMCs from carriers using paired comparative PCR, whereas Galun et al [39] demonstrated immunohistologically that the HBsAg was present in lymphoma cells in about 20% of HBV-positive B-cell ML cases. Kim et al [40] reported that the adjusted odds ratios of HBV infection of 136 patients with B-cell ML were 2.42 versus patients with nonhematopoietic disorders and 4.57 versus patients with nonmalignant conditions in South Korea. In the examined splenic DLBCL cases, the HBV prevalence (20.7%) was significantly ($P < .01$) higher than that of nodal DLBCL (1.9%). By real-time PCP, the 2 examined splenic DLBCL cases had HBV DNA in their tumor tissues and lymphoma cells in 2 of 6 DLBCL cases showed an intranuclear reaction for the HBsAg. The findings support that HBV infection also influences the lymphomagenesis of B cells.

This is the first report regarding the significant prevalence of HCV and HBV infections in splenic DLBCL cases, which mainly show a favorable clinical course after splenectomy and cytotoxic treatments. Type II CG and rearrangement of the *Bcl2* gene in the tumor tissue were not found in the examined cases of HCV-positive splenic DLBCL. Further studies are necessary to identify the effects of HV infections, especially HCV, in splenic DLBCL cases.

References

[1] Ferri C, Caracciolo F, Zignego AL, et al. Hepatic C infection in patients with non-Hodgkin's lymphoma. Br J Haematol 1994;88: 392–4.

[2] Silvestri F, Pipan C, Barillari G, et al. Prevalence of hepatitis C virus infection in patients with lymphoproliferative disorders. Blood 1996;87:4296–301.

[3] De Vita S, Sacco C, Sansonno D, et al. Characterization of overt B-cell lymphomas in patients with hepatitis C virus infection. Blood 1997;90:776–82.

[4] Arcaini L, Paulli M, Boveri E, et al. Splenic and marginal zone lymphoma are indolent disorders at high hepatitis C virus seroprevalence with distinct presenting features but similar morphologic and phenotypic profiles. Cancer 2004;100:107–15.
[5] Hermine O, Lefrere F, Bronowicki JP, et al. Regression of splenic lymphoma with villous lymphocytes after treatment of hepatitis C virus infection. N Engl J Med 2002;347:89–97.
[6] Mizorogi F, Hiramoto J, Nozato A, et al. Hepatitis C virus infection in patients with B-cell non-Hodgkin's lymphoma. Int Med 2000;39: 112–7.
[7] Satoh T, Yamada T, Nakano S, et al. The relationship between splenic malignant lymphoma and chronic liver disease associated with hepatitis C virus infection. Cancer 1997;80:1981–8.
[8] Lymphoma study group of Japanese pathologists. The World Health Organization classification of malignant lymphomas in Japan. Pathol Int 2000;50:696–702.
[9] Sansonno D, De Vita S, Cornacchiulo V, et al. Detection and distribution of hepatitis C virus-related proteins in lymph nodes of patients with type II mixed cryoglobulinemia and neoplastic or nonneoplastic lymphoproliferation. Blood 1996;88:4638–45.
[10] Locatelli GA, Spadari S, Maga G. Hepatitis C virus NS3 ATPase/ helicase. Biochemistry 2002;41:10332–42.
[11] Cocquerel L, Kuo CC, Dubuisson J, Levy S. CD81-dependent binding of hepatitis C virus E1 E2 heterodimers. J Virol 2003;77:10677–83.
[12] Zuckerman E, Suckerman T, Sahar D, et al. The effect of antiviral therapy on t(14;18) translocation and immunoglobulin gene rearrangement in patients with chronic hepatitis C virus infection. Blood 2001;97:1555–9.
[13] Galun E, Livni N, Ketzinei M, et al. Hepatitis B virus infection associated with hematopoietic tumors. Am J Pathol 1994;154:1001–7.
[14] Simmonds P, Holmes EC, Cha TA, et al. Classification of hepatitis C virus into six major genotypes and a series of subtypes by phylogenetic analysis of the NS-5 region. J Gen Virol 1993;74: 2391–9.
[15] Takeuchi T, Katsume A, Tanaka T, et al. Real-time detection system for quantification of hepatitis C virus genome. Gastroenterology 1999;116:636–42.
[16] Zanella I, Rossini A, Domenighini D, et al. Quantitative analysis of hepatitis B virus DNA by real time amplification. Eur J Clin Microbiol Infect Dis 2002;21:22–7.
[17] Jaffe ES, et al, editors. Tumors of haematopoietic and lymphoid tissues. WHO classification of tumors. Lyon: IARC Press; 2001, 121–187.
[18] Saadoun D, Suarez F, Lefrere F, et al. Splenic lymphoma with villous lymphocytes, associated with type II cryoglobulinemia and HCV infection. Blood 2005;105:74–6.
[19] Lunel F, Musset L, Cacoub P, et al. Cryoglobulinemia in chronic liver diseases. Gastroenterology 1994;106:1291–300.
[20] Ivanovski M, Silvestri F, Pozzato G, et al. Somatic hypermutation, clonal diversity, and preferential expression of the *VH* 51 p1/VL kv325 immunoglobulin gene combination in hepatitis C virus associated immunocytomas. Blood 1998;91:2433–42.
[21] Miklos JA, Swerdlow SH, Bahler DW. Salivary gland mucosa–associated lymphoid tissue lymphoma immunoglobulin *VH* genes show frequent use of V1-69 with distinct CDR3 features. Blood 2000;95:3878–84.
[22] Silvestri F, Barillari G, Fanin R, et al. Impact of hepatitis C virus infection on clinical features, quality of life and survival of patients with lymphoplasmacytic lymphoma/immunocytoma. Ann Oncol 1998;9:499–504.
[23] Takeshita M, Sakai H, Okamura S, et al. Prevalence of hepatitis C virus infection in cases of B-cell lymphoma in Japan: histological and etiologic differences of the southern European cases. Histopathology; in press.
[24] Tanaka K, Aiyama T, Imai J, et al. Serum cryoglobulinemia and chronic hepatitis C virus disease among Japanese patients. Am J Gastroenterol 1995;90:1847–52.
[25] Lenzi M, Frisoni M, Mantovani V, et al. Haplotype HLA-B8-DR3 confers susceptibility to hepatitis C virus–related mixed cryoglobulinemia. Blood 1998;91:2062–6.
[26] Nagasaka A, Takahashi T, Sasaki T, et al. Cryoglobulinemia in Japanese patients with chronic hepatitis C virus infection: host genetic and virological study. J Med Virol 2001;65:52–7.
[27] Murakami Y, Hotei H, Tsumura H, et al. A case of primary splenic malignant lymphoma and review of 98 cases reported in Japan. J Jpn Clin Surg 1988;49:716–9.
[28] Dammacco F, Sansonno D, Piccoli C, Tucci FA, Racanelli V. The cryoglobulinemias: an overview. Eur J Clin Invest 2001;31: 628–38.
[29] Bronowicki JP, Bineau C, Feugier P, et al. Primary lymphoma of the liver: clinicopathological features of relationship with HCV infection in French patients. Hepatology 2003;37:781–7.
[30] Luppi M, Ferrari MG, Bonaccorsi G, et al. Hepatitis C virus infection in subsets of neoplastic lymphoproliferations not associated with cryoglobulinemia. Leukemia 1996;10:351–5.
[31] Sakamuro D, Furukawa T, Takegami T. Hepatitis C virus nonstructural protein NS3 transforms NIH 3T3 cells. J Virol 1995;69: 3893–6.
[32] Hofmann WP, Hermann E, Kronenberger B, et al. Association of HCV related mixed cryoglobulinemia with specific mutational pattern of the HCV E2 protein and CD81 expression on peripheral B lymphocytes. Blood 2004;104:1228–9.
[33] Szollosi J, Horejsi V, Bene L, et al. Supramolecular complexes of MHC class I, MHC class II, CD20, and tetraspan molecules (CD53, CD81, and CD82) at the surface of a B cell line JY. J Immunol 1996;157:2939–46.
[34] Ferrer M, Yunta M, Lazo PA. Pattern of expression of tetraspanin antigen genes in Burkitt lymphoma cell lines. Clin Exp Immunol 1998;113:346–52.
[35] Sasso EH, Martinez M, Yarfitz SL, et al. Frequent joining of *Bcl-2* to a *JH6* gene in hepatitis C virus–associated t(14;18). J Immunol 2004;143:3549–56.
[36] Boiocchi M. Low frequency of Bcl-2 rearrangement in HCV-associated non-Hodgkin's lymphoma tissues. Leukemia 2003;17: 1433–6.
[37] Machida K, Cheng KTN, Sung VMC, et al. Hepatitis C virus induces a mutator phenotype: enhanced mutations of immunoglobulin and protooncogenes. Proc Natl Acad Sci 2004;101:4262–7.
[38] Stoll-Becker S, Repp R, Glebe D, et al. Transcription of hepatitis B virus in peripheral blood monoclear cells from persistently infected patients. J Virol 1997;71:5399–407.
[39] Galun E, Ilan Y, Livni N, et al. Hepatitis B virus infection associated with hematopoietic tumors. Am J Pathol 1994;145:1001–7.
[40] Kim JH, Bang Y-J, Part BJ, et al. Hepatitis B virus infection and B-cell non-Hodgkin's lymphoma in a hepatitis B endemic area. A case control study. Jpn J Cancer Res 2002;93:471–7.

臨牀消化器内科 2005 Vol.20 No.5
©日本メディカルセンター

連載

● 薬の知識

アデホビル

加藤　道夫*

はじめに

B型肝炎ウイルス(HBV)キャリアはHBe抗原陽性無症候性キャリアから慢性肝炎，肝硬変，肝細胞癌あるいは臨床的治癒とされているHBe抗体陽性無症候性キャリアまで，さまざまな病態が存在する．そして，その経過もさまざまであるが，大別すると肝硬変，肝細胞癌に進行する群と臨床的治癒の状態に落ち着く群に二分される．約80%は後者になると考えられるが，B型肝癌死亡者数も年間約5,000名を数え，これに肝不全死や劇症化による死亡を加えるとB型肝疾患による死亡者数は年間7,000～8,000名に上ると考えられている．

B型肝疾患の予後改善はHBe抗原が陰性化しHBV-DNA量低値が持続することによって得られ，対象例には適切な抗ウイルス治療がきわめて重要と考えられる．これまでB型慢性肝炎に対する抗ウイルス薬としてはインターフェロンとラミブジンの2薬のみが保険適用薬であったが，2004年12月より新たにアデホビルが保険適用となり，抗ウイルス治療の幅が広がってきた．

I．アデホビルピボキシル

アデホビルは，1986年に発見された核酸誘導体の抗ウイルス薬で，ウイルス遺伝子の複製にDNAポリメラーゼ/逆転写酵素を必要とするHBV，ヒト免疫不全ウイルス(HIV)などのレトロウイルス，ヘルペスウイルスなどに強い抗ウイルス活性を示した．しかし，バイオアベイラビリティが低かったため，ピボキシル基を導入したバイオアベイラビリティの高いアデホビルピボキシル(ヘプセラ® 錠)が合成された．

当初，HIV感染症治療薬，B型慢性肝炎治療薬として開発が開始された[1]が，HIV感染症治療薬としての開発は途中断念され，B型慢性肝炎治療薬として米国で2002年9月に承認された．2004年現在，39カ国で承認されている．

II．安全性

腎機能障害と乳酸アシドーシスおよび脂肪沈着による重度の肝腫大(脂肪肝)が重大な副作用

Key words：アデホビル，アデホビルピボキシル，ラミブジン，B型慢性肝炎，YMDD変異

Michio Kato
*独立行政法人国立病院機構大阪医療センター消化器科(〒540-0006 大阪市中央区法円坂2-1-14)

と考えられる．本剤投与中は腎機能障害の発現に注意し，とくに，腎機能障害のある患者やその既往歴のある患者においては，血清クレアチニンおよび血清リンの変動を定期的に観察する必要がある．国内第III相臨床試験(36例)における副作用としては悪心嘔吐，背部痛，NAG増加およびALP増加が各1例報告されている[2]．

III．臨床効果

アデホビルはYMDD野生株に対する有効性も報告されている[3]が，現在，本邦での保険適用はラミブジン投与中にHBVの持続的な再増殖を伴う肝機能の異常が確認されたB型慢性肝炎およびB型肝硬変例である．国内第III相臨床試験[2](16週投与)においてHBV-DNA変化量はラミブジンとの併用投与によって，16週後−3.75 log 10 copies/m*l*と著明に減少した(**図1**)．またALT正常化率も16週後に72%(26/36)と高率であった(**図2**)．耐性ウイルスに関しては少数報告されている[4),5)]が，これらはラミブジンに対して感受性をもっているので，ラミブジンとの併用時には大きな障害にはならないと考えられる．

IV．症　例

アデホビル投与が有効であったHBe抗原陽性B型慢性肝炎の1例を呈示する(**図3**)．

HBステージ[6]IIb．ラミブジン投与前の肝組織診断は新犬山分類A2F3．投与直前のHBV-DNA量は3.5 Meq/m*l*，ALTは126 IU/*l*であった．

2000年7月11日よりラミブジン150 mg/dayを開始，2001年2月より100 mg/dayとし，現在まで続行中である．HBV-DNA量は速やかに低下し，2001年9月にPCR法で感度以下となった．その後，順調に経過していたが，2002年2月ごろより，HBV-DNA量の増加が持続し，2002年3月にYMDD変異株(YIDD)の出現を確認した．同時期よりALTの上昇とともに血清アルブミン値が低下し始め，同年11月には2.6 g/d*l*まで低下し，その状態が持続したため，2003年4月21日より個

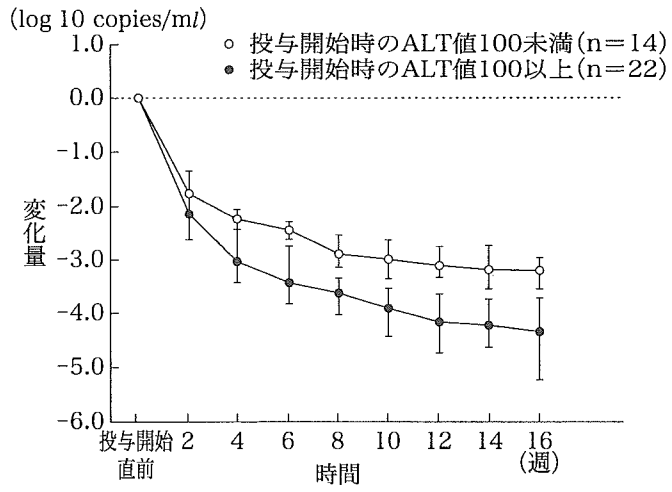

図1　アデホビル投与開始時のALT値別HBV-DNA変化量(国内第III相臨床試験)

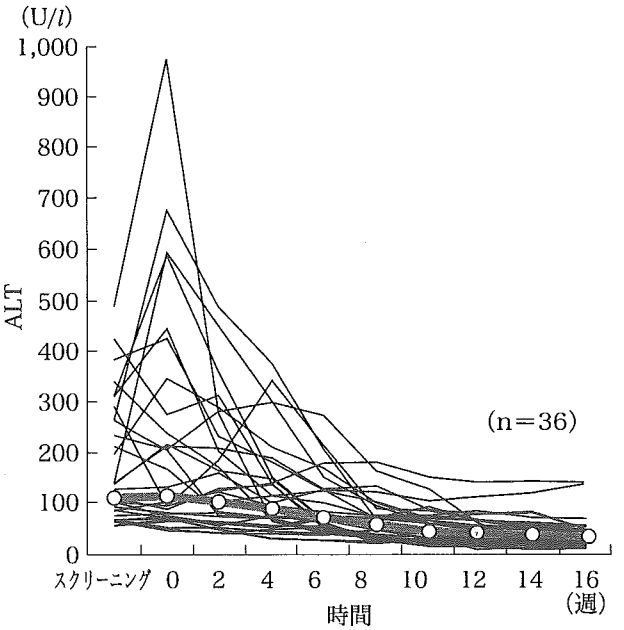

図2　アデホビル投与期間中のALT値の推移(国内第III相臨床試験)

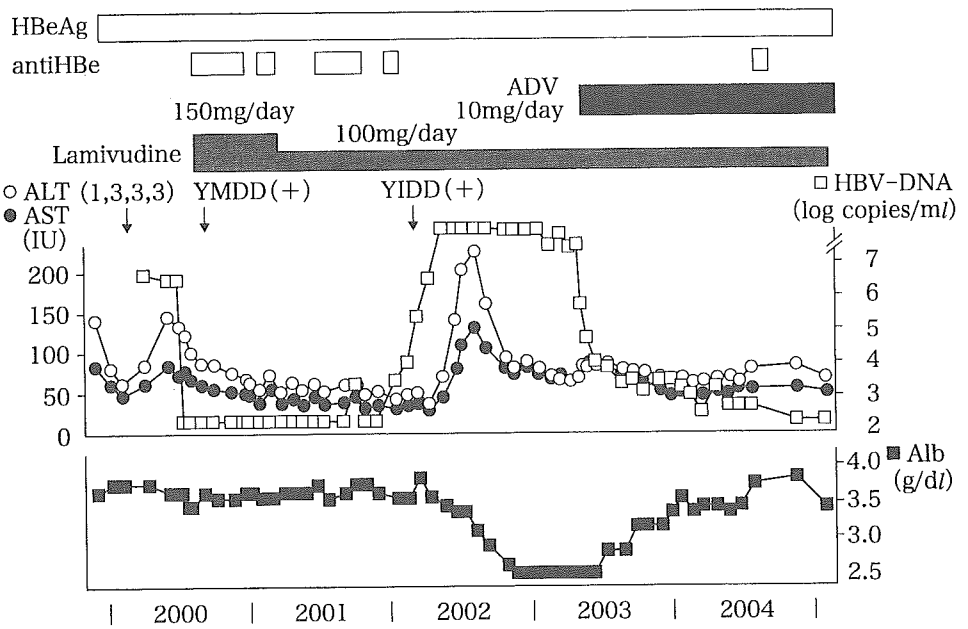

図3 アデホビル投与が有効であったYMDD変異株出現B型慢性肝炎例

人輸入にてアデホビル10 mg/dayの投与を開始した.

HBV-DNA量はアデホビル投与開始時7.2 log copies/m*l*であったが, 投与1カ月後4.7, 2カ月後3.9, 6カ月後3.3と低下し, 2004年9月より感度以下が持続している. 血清アルブミン値もアデホビル投与開始時2.6 g/d*l*であったが, 2カ月後2.9, 6カ月後3.3と増加し, 2004年10月には4.0 g/d*l*まで増加した. HBe抗原価もアデホビル投与開始後, 漸次低下し, 最終観察時点で3.9 C.O.Iとなり, HBe抗原の陰性化が期待できる状態である.

V. YMDD変異株出現とbreakthrough hepatitis

前述の症例ではYMDD変異株出現に伴って, いわゆるbreakthrough hepatitisが生じたが, HBV-DNA量の増加は認められるが, AST, ALTは正常値が持続し, breakthrough hepatitisを起こさない例やYMDD変異株が出現してもHBV-DNA量がほとんど増加しない例も存在する. breakthrough hepatitisが生じた群をA群, HBV-DNA量の増加は認められるがbreakthrough hepatitisを起こさない群をB群, YMDD変異株が出現してもHBV-DNA量がほとんど増加しない群をC群とすると, A群, B群ではHBVのRNA依存性DNAポリメラーゼのC-ドメインの変異(YVDD, YIDD)とともにB-ドメイン180番目のロイシンからメチオニンへの変異がきわめて高頻度で認められるが, C群ではC-ドメインの変異のみであることが多い.

A群とB群の判別は現在, 明らかではないが, 時期の問題か, 生体側の因子が関係している可能性が考えられる. C-ドメインの変異(YVDD, YIDD)が認められたら, 慎重に経過を観察し, breakthrough hepatitis増悪時には速やかなアデホビルの導入を考慮する必要がある.

おわりに

B型慢性肝炎でHBe抗原陽性持続例やHBe抗原は陰性化してもHBV-DNA量5.0 log copies/m*l*以上が持続する例は発癌リスクが高く[6]，抗ウイルス治療の導入が必要となる．ラミブジン治療においてはYMDD変異株の高頻度の出現が導入を逡巡させる一因であったが，アデホビルがB型慢性肝炎治療の選択肢に加わったことで，抗ウイルス治療の安全性と利便性が大きく広がったと考えられる．

文　献

1) Deeks, S. G., Collier, A., Lalezari, J., et al.：The safety and efficacy of adefovir dipivoxil, a novel anti-human immunodeficiency virus(HIV)therapy, in HIV-infected adults：a randomised, double blind, placebo-controlled trial. J. Infect. Dis. 176；1517-1523, 1997
2) 谷川久一，熊田博光，佐田通夫，他：YMDD変異ウイルスの増殖により肝機能の異常が認められたB型慢性肝炎患者(B型肝硬変患者を含む)に対するヘプセラ錠(アデホビルピボキシル)の臨床効果．肝胆膵　50；193-211, 2005
3) Marcellin, P., Chang, T. T., Lim, S. G., et al.：Adefovir dipivoxil for the treatment of hepatitis B e antigen-positive chronic hepatitis B. N. Engl. J. Med.　348；808-816, 2003
4) Angus, P., Vaughan, R., Xiong, S., et al.：Resistance to adefovir dipivoxil therapy associated with the selection of a novel mutation in the HBV polymerase. Gastroenterology　125；292-297, 2003
5) Villeneuve, J. P., Durantel, D., Durantel, S., et al.：Selection of a hepatitis B virus strain resistant to adefovir in a liver transplantation patient. J. Hepatl.　39；1085-1089, 2003
6) 加藤道夫，伊与田賢也，結城暢一，他：HBVマーカーと発癌リスクよりみたHBVキャリアのステージ分類―適切な抗ウィルス治療の選択に向けて．肝臓　45；581-588, 2004

特集

B型慢性肝炎治療の最前線
インターフェロン療法

Interferon therapy for chronic hepatitis B

加藤　道夫
KATO Michio

Key words　IFN治療　HBステージ分類　IFN・ラミブジン併用治療　ペグIFN治療　長期予後

HBVキャリアはHBe抗原陽性無症候性キャリアから慢性肝炎，肝硬変，肝細胞癌あるいは臨床的治癒とされているHBe抗体陽性無症候性キャリアまでさまざまな病態が存在する．そして，その経過もさまざまであるが，大別すると肝硬変，肝細胞癌に進行する群と臨床的治癒の状態に落ち着く群に二分される．約80%は後者になると考えられるが，B型肝癌も全肝細胞癌中10～15%を占め，現在，死亡者数は横ばいで年間約5,000名を数えている．これに，肝不全死や劇症化による死亡を加えるとB型肝疾患による死亡者数は年間7,000名～8,000名に上ると考えられる．B型慢性肝炎の予後改善にはHBe抗原の陰性化とHBV-DNAの低値持続が必要であり，そのためには適切な抗ウィルス治療が肝要となる．現在，インターフェロン(IFN)，ラミブジンおよびアデホビルが保険適用製剤であるが，本稿ではB型慢性肝炎に対するIFN治療の現状と今後の展望について述べる．

Ⅰ．HBVキャリアのステージ分類とIFN治療対象の位置づけ

われわれはB型慢性肝炎の肝硬変進展，肝癌発癌抑止を目的とした適切な抗ウィルス治療の選択に向けての，HBVマーカーと発癌リスクよりみたHBVキャリアのステージ分類を提唱した[1]（表1）．

独立行政法人大阪医療センター消化器科　部長

HBステージ0

HBs抗原陽性，HBe抗原陽性，ALT正常値持続のいわゆる無症候性キャリアの状態．発癌リスクはほとんどなく，抗ウィルス治療の適応なし．

HBステージⅠ

HBs抗原陽性，HBe抗原陽性，ALT異常値(持続正常以外)でHBV-DNA量が$10^{7.6}$copies/mL以上の高ウィルス群．若年例(男性：30歳未満，女性：35歳未満)をステージⅠa，高年例(男性：30歳以上，女性：35歳以上)をステージⅠbとする．ステージ1a群も発癌リスクがきわめてまれで，

0371-1900/05/¥50/頁/JCLS

表1 HBVキャリアのステージ分類

HB stage	0	Ⅰ	Ⅱ	Ⅲ	Ⅳ	Ⅴ
HBsAg	＋	＋	＋	＋	＋	**－
HBeAg	＋	＋	＋	－	－	－
HBV-DNA (copies/ml)	不問	$10^{7.6}$≦	$10^{7.6}$＞	10^{5}≦	10^{5}＞	不問
ALT	持続正常	*持続正常以外	*持続正常以外	不問	不問	不問
年齢	不問	若年/高年 (Ⅰa/Ⅰb)	若年/高年 (Ⅱa/Ⅱb)	不問	不問	不問
発癌リスク	きわめて小	小/大	小/きわめて大	きわめて大	きわめて小	きわめて小

*若年：男性30歳未満，女性35歳未満　** HBsAg(＋)の時期が確認されていること
高年：男性30歳以上，女性35歳以上

通常は抗ウィルス治療の必要はないが組織学的に線維化ステージが進行している例は抗ウィルス治療の適応となる．ステージⅠa，Ⅱaとも薬剤としては若年で免疫応答が良好であるのでIFNが第一選択となると考える．IFNについてわれわれは後述の少量間歇投与が若年例に有効であることを報告[2]したが，特に30歳未満例にはIFN治療は長期投与でなくても有効性は高いと考える．一方，ステージⅠb群は発癌リスクを有し，抗ウィルス治療の必要を認める．HBV-DNA量がきわめて高値のこの群はラミブジン単独での治療効果の持続は困難で，エンテカビル等の抗ウィルス効果の強い薬剤あるいはIFN/ラミブジン併用治療が適応になると考えられる．

HBステージⅡ

HBs抗原陽性，HBe抗原陽性，ALT異常値(持続正常以外)でHBV-DNA量が$10^{7.6}$copies/mL未満の低ウィルス群．若年例をステージⅡa，高年例をステージⅡbとする．ステージⅡa群は発癌リスクは少ないが若年発癌例が存在し，またALT高値が持続する例も多く，抗ウィルス治療の適応になる．ステージⅡb群は発癌リスクがきわめて大で抗ウィルス治療の絶対適応である．ラミブジン等の核酸アナログ単独あるいはIFN，HBワクチンとの併用の選択が考えられる．

HBステージⅢ

HBs抗原陽性，HBe抗原陰性，HBV-DNA 10^{5}copies/mL以上のpre-core mutant株のreplicationが持続している群である．発癌リスクはきわめて大で，ALT値異常のとくに男性はステージⅡbとともに抗ウィルス治療の絶対適応である．薬剤としては高年例が大半を占め，ラミブジンの治療効果が良好でYMDD変異株の出現も低率であるため，現在のところラミブジンが第一選択であり，YMDD変異株出現例にはアデホビル等の他の核酸アナログの併用あるいは切り替えで対応できると考えられる．

HBステージⅣ

HBs抗原陽性，HBe抗原陰性，HBV-DNA 10^{5}copies/mL未満のいわゆる臨床的治癒の状態である．発癌リスクとしてはきわめてまれで原則的には抗ウィルス治療の必要はないと考える．

HBステージⅤ

HBキャリア(HBs抗原陽性の時期が確認されている例)でHBs抗原が消失した状態である．HBステージⅣと同様，発癌リスクはきわめてまれで抗ウィルス治療の必要はない．

HBVキャリアの大多数が歩む臨床的治癒状態へのコースはステージⅠaからステージⅡaとなり，その後短期間ステージⅢを経由した後速やかにステージⅣに移行するものと考えられる．そしてステージⅣが長期間続いた後HBs抗原が消失し，ステージⅤとなる．一方，肝硬変進展・肝癌発癌ハイリスク群はステージⅠaからステージ

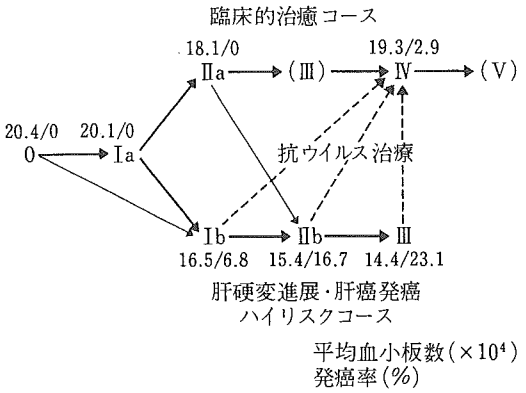

図1　HBV キャリアの経過(臨床的治癒コースと肝硬変進展・肝癌発癌ハイリスクコース)

Ⅰb，ステージⅡb と進行し，HBe 抗原が陰性化してステージⅢまでは到達するが HBV の増殖は持続し，ステージⅣに至ることはない(図1)．臨床的治癒コースの各ステージにおける初診時の血小板数と発癌リスクは，ステージ0，Ⅰa，ⅡaおよびⅣでそれぞれ20.4万/0%，20.1万/0%，18.1万/0%および19.3万/2.9%とほとんど変化を認めないが，肝硬変進展・肝癌発癌ハイリスクコースにあたるステージⅠb，Ⅱb およびⅢではそれぞれ16.5万/6.8%，15.4万/16.7%および14.4万/23.1%とステージの移行にしたがっての血小板数の低下と発癌率の増加が認められ，ステージⅠb，Ⅱb およびⅢのキャリアに対する抗ウィルス治療の必要性が強く示唆される．特に IFN 治療の適用対象としては，HBe 抗原陽性若年例(ステージⅠa，Ⅱa)では IFN 単独，HBe 抗原陽性高年例(ステージⅠb，Ⅱb)では IFN/ラミブジン併用治療(後述)が適切な選択ではないかと考える．

Ⅱ．これまでの IFN 治療

1．少量間欠投与

われわれは1984年より HBe 抗原陽性例に対して natural IFNαの少量間欠投与を行い，良好な成績を報告[2]した．投与法は大阪府赤十字血液センターより供与をうけたヒト白血球 IFN を週1回計4回(初回量2.4MU～3MU，以下漸減投与)総量6.8MU～10MU の投与である．投与対象の性別は男性9例，女性6例で，それぞれの年齢は男性20歳～55歳(平均35.8歳)，女性22歳～45歳(平均31.7歳)であった．成績は投与終了後6ヵ月での HBe 抗原陰性化率53.3%(図2)，HBe 抗原抗体 seroconversion 率33.3%および ALT 正常化率53.3%といずれも高率であった．HBe 抗原陰性化例の多くは投与終了後，ALT の上昇後に消失し，女性，HBe 抗原価低値，投与前 ALT 高値および組織診断で activity の高い症例に得られやすいことが判った．対象の60%が35歳未満の若年であったことが良好な成績が得られた要因と考えられ，HB ステージⅠa，Ⅱa で抗ウィルス治療

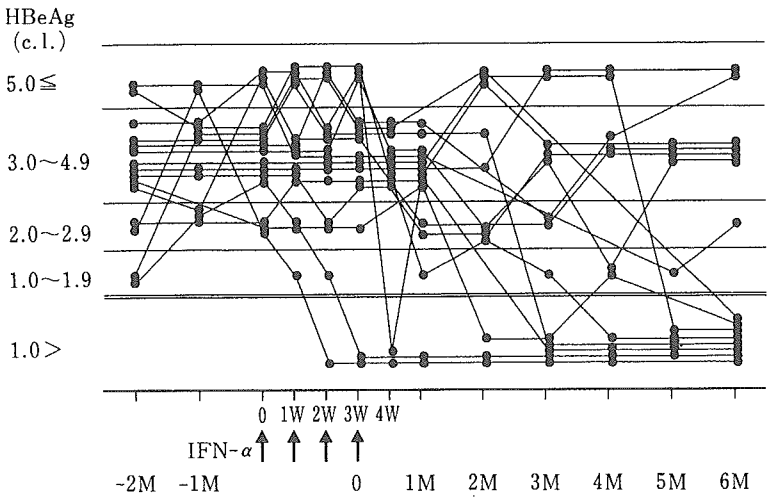

図2　IFN 少量間欠投与前後の HBe 抗原カットオフインデックスの変動